DOI 10.1002/mawe.201300051

The interaction of epoxy adhesives with steel surfaces

Wechselwirkungen von Epoxid-Klebstoffen mit Stahloberflächen

H. Munkert[1,2], F. Voigts[3], L. Wegewitz[1,4], H. Palkowski[2,4], W. Maus-Friedrichs[1,4]

Deformable sandwich sheet materials have the advantage to be produced as raw materials and to be formed afterwards to even complex geometries. Moreover they are cost effective and predestinated for mass production. For such systems the necessity is given for a good bonding to guarantee a good shear transfer between the single layers. Because of deformation, failures by delamination often occur at the interface between the metal and the epoxy layer. Therefore investigations at this interface were performed using Atomic Force Microscopy (AFM) and X-ray Photoelectron Spectroscopy (XPS), to understand the basic effect of the surfaces' bonding behavior in selected preparation steps of the system. Basic information about the adhesion mechanisms between the stainless steel 316L and the epoxy is given. The chemical interaction between the epoxy and the steel results in a significant reduction of Fe^{3+} to Fe^{2+}.

Keywords: Metal Epoxy Hybrids / Adhesion Layer / Delamination / Atomic Force Microscopy / X-ray Photoelectron Spectroscopy

Umformbare Sandwichverbunde haben den Vorteil, als Halbzeug hergestellt werden zu können, um im weiteren Prozessablauf dann umformtechnisch ihre durchaus auch komplexe Endform zu erhalten. Somit sind sie kostengünstig und für die Massenproduktion prädistiniert. Für solche Systeme ist eine gute Verbindung zwischen den einzelnen Sandwichschichten unabdingbar, um eine gute Schub- und Kraftübertragung zu garantieren. Aufgrund der plastischen Deformation bei der Umformung kann es zu Versagen durch Delamination an der Grenzfläche zwischen Metall und Epoxidkleber kommen. Um die grundlegenden Effekte des Bindungsverhaltens in solchen Systemen zu verstehen, wurden Untersuchungen mittels Rasterkraftmikroskopie (AFM) und Röntgen-Photoelektronenspektroskopie (XPS) durchgeführt. Es werden grundlegende Informationen zu Adhäsionsmechanismen zwischen dem verwendeten Edelstahl 316L und dem Epoxidkleber dargelegt. So ließ sich z. B. die Reduktion von Fe^{3+} zu Fe^{2+} bei der Wechselwirkung der einzelnen Materialien miteinander nachweisen.

Schlüsselwörter: Metall-Epoxid-Verbund / Adhäsionsschicht / Delamination / Rasterkraftmikroskopie / Röntgen-Photoelektronenspektroskopie

1 Introduction

The demand to integrate functional properties and design a part to its needs make it necessary to use the specific properties of mono-materials and combine them to hybrid materials with improved properties compared to the mono-materials. Following Kickelbick, a "hybrid material is used for many different systems across a wide area of different materials such as crystalline highly ordered coordination polymers, amorphous sol-gel compounds, and materials with and without interactions between the inorganic and organic unit" [1]. Therewith the goal of lightweight structures with high strength and stiffness and good damping properties can be achieved as well as low density, high energy absorption and high load capacity, properties not to be reachable by the single mono-materials alone [2, 3].

1.1 State of research

A sandwich construction is the combination of a lightweight material with a stronger – and in general heavier – one, where the lighter one generally deals as an intermediate core layer [4]. The soft core defines the distance between the cover layers, supports the metal sandwich skins under load, dissipating the shearing forces. The core material can be made of polymer foils or foams, balsa wood, paper or polymer or metal honeycombs [5].

[1] Institut für Energieforschung und Physikalische Technologien, Technische Universität Clausthal, Leibnizstraße 4, 38678 Clausthal-Zellerfeld, Germany
[2] Institut für Metallurgie, Technische Universität Clausthal, Robert-Koch-Straße 42, 38678 Clausthal-Zellerfeld, Germany
[3] Institut für Mechanische Verfahrenstechnik, Technische Universität Clausthal, Arnold-Sommerfeld-Straße 6, 38678 Clausthal-Zellerfeld, Germany
[4] Clausthaler Zentrum für Materialtechnik, Technische Universität Clausthal, Leibnizstraße 4, 38678 Clausthal-Zellerfeld, Germany

Corresponding author: Wolfgang Maus-Friedrichs, Institut für Energieforschung und Physikalische Technologien, Technische Universität Clausthal, Leibnizstraße 4, 38678 Clausthal-Zellerfeld, Germany
E-mail: w.maus-friedrichs@pe.tu-clausthal.de

They are in use in various combinations of skins such as carbon, glass and/or fibre-reinforced polymers, as well as aluminum, titanium or steel. The single layers are usually connected in a bonding process by gluing, welding or mechanical/chemical reactions. Using steel as cover sheets and a polypropylene foil between the steel sheets generates a weight reduction of about 50% – keeping the same stiffness of a comparable steel sheet. With the use of stainless steel as cover sheet an improved corrosion resistance can be achieved. Moreover these types of steel show a high level of elongation to fracture and a good ratio for complex shaping geometries.

Besides the plastic materials and their combination to hybrids – which are often not deformable after curing and therewith have to be structured by placing layer by layer in a batch process – those sandwich structures are of specific interest, especially for mass production, since they can be produced as raw materials and shaped by standard forming machines into their final structure. They find their application in a wide spread area from white ware and construction over the wide field of automotive, naval industries, to aircraft and even space industries.

The bond strength between the single layers depends on the level of the bondability between the single materials and their adhesion [6]. The adhesion between two materials is influenced by the conditions of bonding as well as the surface quality and the chemical conditions. To understand the adhesive bonding of metal polymer sandwiches different theories were presented. The mechanical adhesion by micromechanical anchorage and the auto-adhesion by the diffusion of macro molecules are based on simple mechanisms while the specific adhesion can be linked to physical-chemical and thermodynamic phenomena. De Bruyne describes the interactions between functional groups of adherents and adhesive, based on the electrical polarity of the atoms or the molecular groups [7]. To improve the adhesion of both, the adherents and the adhesives, the polymer must contain polar groups and present dipoles. In comparison to other theories based only on physical bonds between adherent and components, the "Chemical adhesion model" assumes that not only intermolecular forces but also chemical sorption can occur [8].

1.2 Materials

For the present experiments, the stainless steel sheet material 316L – X2CrNiMo17-12-2 – and the one-component epoxy resin Köratac FL 201 were chosen as components of the sandwich laminate of [9, 10]. This sandwich consists of polymeric layers (polyolefin foil PP-PE) and metallic layers that were bonded together by roll bonding using the epoxy resin. In the standard manufacturing process of such sandwich laminates the adhesive was activated at (260 ± 2) °C on the steel surface before roll bonded with the PP-PE foil.

For standard deep drawing processes with moderate deformations the sandwich could be shaped without failure. Nevertheless delamination occurred under high ratios of deformation [11].

To improve the bonding between metal and organic component the mechanisms of bonding have to be understood. Since those mechanisms can be traced back to changes at the metal-organic interface the investigation of such changes is essential. The determination of topographical changes is realized by Atomic Force Microscopy, while X-ray Photoelectron Spectroscopy is applied to examine changes in chemical composition and chemical bonding. The acquired knowledge may clear up the way for the optimization of surface pretreatments and choice of materials for improved bonding strength in sandwich structures.

2 Experimental

X-ray Photoelectron Spectroscopy, a powerful method in surface chemistry and surface physics, is applied to analyze the chemical composition as well as chemical bonds at the surfaces. The experiments are performed in an ultrahigh vacuum apparatus (Omicron Multiprobe) with a base pressure of 1×10^{-10} hPa using a hemispherical analyzer (Omicron EA 125) in combination with a non-monochromatic X-ray source (Omicron DAR 400). During X-ray Photoelectron Spectroscopy measurements, X-ray photons hit the surface under an angle of 45 ° to the surface normal. For all measurements presented here, the Al K_α line with a photon energy of 1486.6 eV is used. Electrons are recorded by the hemispherical analyzer with a calculated analyzer resolution of 0.83 eV for detail spectra and 2.07 eV for survey spectra. The analyzer is mounted at an angle of 45 ° to the surface normal, analyzing a spot of about 1.5 mm in diameter. All X-ray Photoelectron spectra are displayed as a function of electron binding energy with respect to the Fermi level.

For quantitative X-ray Photoelectron Spectroscopy analysis, background substraction according to Shirley is employed [12]. Photoelectron peak areas are calculated via mathematical fitting with Gauss-type profiles using OriginPro 7G including the PFM fitting module, which applies Levenberg-Marquardt algorithms to achieve the best agreement possible between experimental data and fit. Photoelectric cross-sections calculated by Scofield [13], inelastic mean free paths calculated by Seah and Dench [14], asymmetry parameters calculated by Reilman [15] and the transmission function of the hemispherical analyzer are taken into account when calculating stoichiometry. All Fe2p fits were performed using the peak positions and FHWMs published by Volgmann et al. [16] and Lin et al. [17]. The good reproducibility of the experiments allows to estimate the typical deviation in the present results to be certainly below 10%.

For all X-ray Photoelectron Spectroscopy experiments, the sample is mounted on a molybdenum holder and transferred into the UHV by means of a three-stage sample transfer system within 2 h.

Atomic Force Microscopy belongs to the group of Scanning Probe Microscopy Methods. The surface topography is scanned by measuring the atomic forces between a microscope tip and the surface. The topography and roughness of the uncovered steel surfaces, as well as the epoxy covered samples are determined by Atomic Force Microscopy using a Veeco Dimension 3100 SPM. All measurements are performed in Tapping Mode with Al-coated silicon cantilevers (NSC15, MicroMasch). The typical resonant frequencies of this series are about 325 kHz, typical spring constants are in the range of 40 N/m. The radius of the tip curvature is less than 10 nm. All images consist of 512 lines each containing 512 pixels. They are recorded

Table 1. Chemical composition of pure 316L-steel (manufacturer's inscription).

Tabelle 1. Chemische Zusammensetzung des unbehandelten Stahls (Herstellerangabe).

element	Si	P	C	Mo	N	Cr	Mn	Fe	Ni
at.–%	1.7	0.1	0.1	1.2	0.4	18.5	2.0	65.2	10.8

with a line-scan frequency of 0.5 Hz. SPIP (Image Metrology A/S) is used for the depiction of the Atomic Force Microscopy images and the calculation of the root mean square surface roughness according to ISO 4287/1. The recording of one image typically requires 17 min.

The steel samples were cut from a 700×700 mm^2 steel sheet and polished with a grain size of 1 μm. Before introducing them into the vacuum they were cleaned as described below, part a). Besides iron the main alloy components are chromium and nickel. The chemical composition is shown in *Table 1*.

The chemical composition of the epoxy adhesive (Kömmerling Chemische Fabrik GmbH, Köratac FL 201) is unknown in detail. It mainly consists of five different solvents.

Three different surfaces were prepared and analyzed for the investigation of the epoxy – steel interaction:

a) The pure steel surface was manually cleaned with acetone and isopropanol. After this procedure the sample was transferred into the vacuum chamber immediately.

b) The sample from step one was extracted from vacuum and exposed to ambient air for 2 min. This is the time which is required to produce an epoxy layer on the steel surface. Afterwards the sample is transferred into the vacuum system immediately. The investigation of the steel surface before the contact with the epoxy adhesive will serve as a reference state for the examination of possible changes after the epoxy-steel contact.

c) The sample from step two is covered with an epoxy film by spin coating (text below) before being transferred to the vacuum chamber.

Before analyzing, the surfaces of all samples were sputtered by Ar^+ impact at 3 keV kinetic energy for 15 min with target currents of 10 μA using a commercial ion gun (Omicron ISE 5). In this way the majority of the surface contaminations were removed. Spin-coating with epoxy is performed using home-built equipment. The sample was fixed on an electromotive powered rotary holder and a drop of liquid epoxy adhesive was applied to the steel surface. Rapid spinning (about 16.000 min^{-1}) produced a flat film on the steel surface. The spin coating procedure took about 7 min, with the first two accounted for the outward transfer of the sample from the UHV, one for the spin coating itself and the remaining four for the transfer back into the transfer system.

3 Results and discussion

Due to the fact that the Atomic Force Microscope is operated in ambient air, it is impossible to examine a sputtered sample (a) which is not exposed to air. Therefore the discussion is limited to one sample prepared as described in step (b) and a second one prepared as described in step (c) concerning Atomic Force Microscopy.

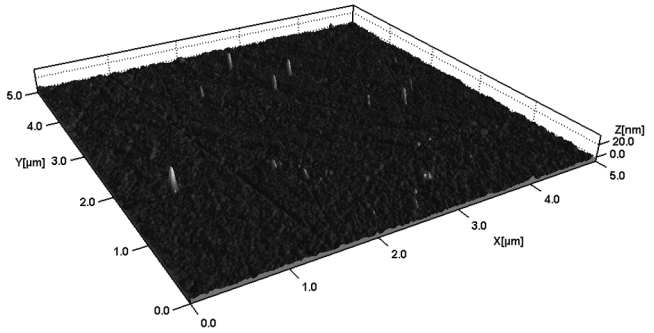

Figure 1. Atomic Force Microscopy image of the sputtered steel surface (5×5 μm^2) exposed to ambient atmosphere. Please refer to the text for details. The vertical axis is magnified by the factor 10.

Bild 1. Rasterkraftmikroskopieaufnahme der Argon-gesputterten Stahloberfläche, die der Umgebungsluft ausgesetzt wurde (Ausschnittsgröße: 5×5 μm^2). Details werden im Text näher erläutert, die vertikale Achse ist um den Faktor 10 vergrößert dargestellt.

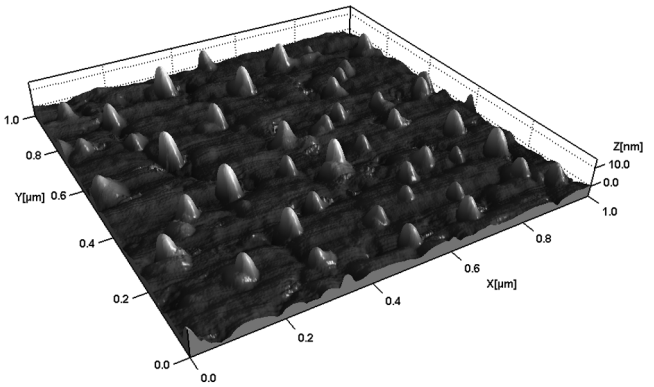

Figure 2. Atomic Force Microscopy image of the sputtered steel surface (1×1 μm^2) exposed to ambient atmosphere, revealing a section with high particle density. The vertical axis is magnified by the factor 5.

Bild 2. Rasterkraftmikroskopieaufnahme der gesputterten und der Luft ausgesetzten Stahloberfläche (Ausschnittsgröße: 1×1 μm^2). Die vertikale Achse ist um den Faktor 5 vergrößert dargestellt.

An Atomic Force Microscopy image (5×5 μm^2) of the sputtered and air exposed steel surface (step (b)) is depicted in *Figure 1*. The section exhibits a smooth surface with a root mean square roughness of 1.5 nm. However there are several distinct structures on the surface. The diameter of those particles ranges from 50 to 150 nm while the mean height amounts to 30 nm. Indicated by their dimensions, the particles are probably aerosols attached to the surface due to the exposure to ambient air.

In order to obtain detailed information about the aerosol particles another position with higher particle density is chosen for imaging, *Figure 2*. Aerosol particles with an average diameter of

Table 2. Chemical composition of the steel surface after different treatments determined by X-ray Photoelectron Spectroscopy (Figure 2).

Tabelle 2. Mit Röntgen-Photoelektronenspektroskopie bestimmte chemische Zusammensetzung der Stahloberfläche nach den verschiedenen Behandlungsschritten (Bild 2).

element (orbital)		Ar(2p)	C(1s)	Mo(3p)	O(1s)	Cr(2p)	Mn(2p)	Fe(2p)	Ni(2p)
electron binding energy [eV]		242	285	394	531	574	639	707	853
(a)	**at.–%**	3.6	15.1	3.2	7.3	9.2	9.1	45.9	6.7
(b)		–	26.6	–	47.7	2.4	2.4	19.5	1.4
(c)		–	81.9	0.5	16.4	0.5	–	0.7	–

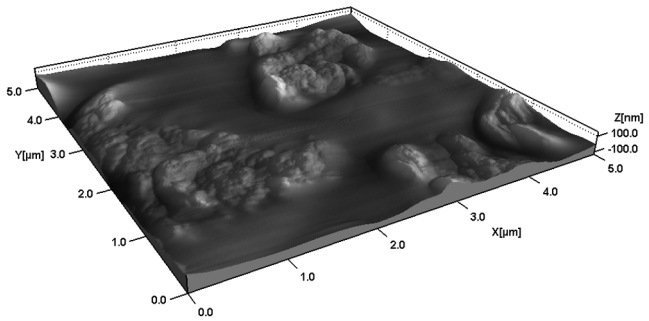

Figure 3. Atomic Force Microscopy image of the sputtered and air exposed steel surface coated with an epoxy layer ($5 \times 5\ \mu m^2$). The vertical axis is magnified by the factor 2.

Bild 3. Rasterkraftmikroskopieaufnahme einer gesputterten und der Luft ausgesetzten Stahloberfläche, die mit einer Epoxidschicht belegt wurde (Ausschnittsgröße: $5 \times 5\ \mu m^2$). Die vertikale Achse ist um den Faktor 2 vergrößert dargestellt.

129 nm and mean height of about 28 nm are found. It is well known, that aerosol particles arising from agglomeration within the atmosphere show a typical size of 100 nm [18].

A section ($5 \times 5\ \mu m^2$) of the sputtered steel surface which has been spin-coated with epoxy (step (c)) is depicted in *Figure 3*. Two different domains can be identified, regions with a comparatively smooth surface where the epoxy appears to be almost uniformly distributed and regions which exhibit noticeable aggregation of epoxy. Therefore the root mean square roughness of the epoxy-coated steel surface amounts to 34 nm.

The corresponding X-ray Photoelectron Spectroscopy survey spectra in the energy range between 0 eV and 1100 eV are shown in *Figure 4*. The relative contributions of the respective elements are comprised in *Table 2*. After the cleaning procedure (a) the surface consists mainly of iron (45.9%) and the alloy components molybdenum (3.2%), chromium (9.2%), manganese (9.1%) and nickel (6.7%). Those values reveal an enrichment of molybdenum and especially manganese in the surface region thus reducing the relative amounts of chromium, nickel and iron. The enrichment can be traced back to the amount of the Gibbs free energy which is the lowest for MnO among the potential metal compounds (–362,9 kJ/mol) [19]. It is well known, for example from chromium in stainless steel, that the chromium surface enrichment follows the reduction of surface oxides by bulk chromium atoms. Probably a comparable process takes place with manganese. Furthermore carbon (15.1%) and oxygen (7.3%) are present at the surface. The oxygen arises from the contamination by the residual atmosphere and oxidic species at the surface. The carbon mainly arises from surface contamination but is also a steel alloy element, Table 1. The small argon contribution can be traced back to the sputter process.

Table 3. Summarized values of all C1s-measurements (underlined values indicate assumed constraints).

Tabelle 3. Zusammenfassung der C1s-Messergebnisse (unterstrichene Werte kennzeichnen vorausgesetzte Zwangsbedingungen).

Preparation	Figure	Peak	C1s				Assignment
			$E_{binding}$ [eV]	ΔE	FWHM	rel. int.	
(a)	**5a**	C_0	283.4	–1.6	**1.6**	46.3	carbide
		C_1	285.0	0	**1.6**	38.1	C-C / C-H
		C_2	286.5	1.5	**1.6**	11.4	C-O
		C_3	287.9	2.9	**1.6**	4.2	C=O
		C_4	–	–	–	–	–
(b)	**5b**	C_0	283.8	–1.8	**1.6**	7.6	carbide
		C_1	285.6	0	**1.6**	50.4	C-C / C-H
		C_2	287.0	1.4	**1.6**	22.4	C-O
		C_3	–	–	–	–	–
		C_4	289.3	3.7	**1.6**	19.6	C=O
(c)	**5c**	C_0*	–	–	–	–	–
		C_1*	286.2	0	**1.7**	54.2	C-C / C-H
		C_2* & C_3*	287.9	1.7	**1.7**	38.0	C-O & epoxy
		C_4*	289.5	3.3	**1.7**	7.8	C=O

The X-ray Photoelectron Spectroscopy survey spectrum of the steel surface after exposing to the ambient atmosphere is shown in Figure 4b. Obviously the amounts of carbon and oxygen are enriched. C1s increases from 15.1% to 26.6% and O1s from 7.3% to 47.7%. In contrast, the metal components are significantly decreased, Mn2p from 9.1% to 2.4%, Cr2p from 9.2% to 2.4%, Ni2p from 6.6% to 1.4%, and Fe2p from 45.9% to 19.5%. All these values are summarized in Table 2.

The X-ray Photoelectron Spectroscopy survey spectrum of the investigated sample after expoy spin coating (step (c))is shown in Figure 4c. The sample surface consists mainly of carbon (81.9%) and oxygen (16.4%). The amounts of metals (Cr2p with only 0.5%, Fe2p with only 0.7% and Mo3p with only 0.5%) are considerably reduced and are close to the X-ray Photoelectron Spectroscopy detection limit. This observation is due to the attenuation of the electrons from the underlying metal substrate during their passage through the epoxy layer. From this attenuation the average epoxy thickness is estimated to 7 ± 2 nm.

The X-ray Photoelectron Spectroscopy detail spectra of the C1s range between 280 eV and 292 eV is shown in *Figure 5*. The relative contributions of different carbon species are comprised in

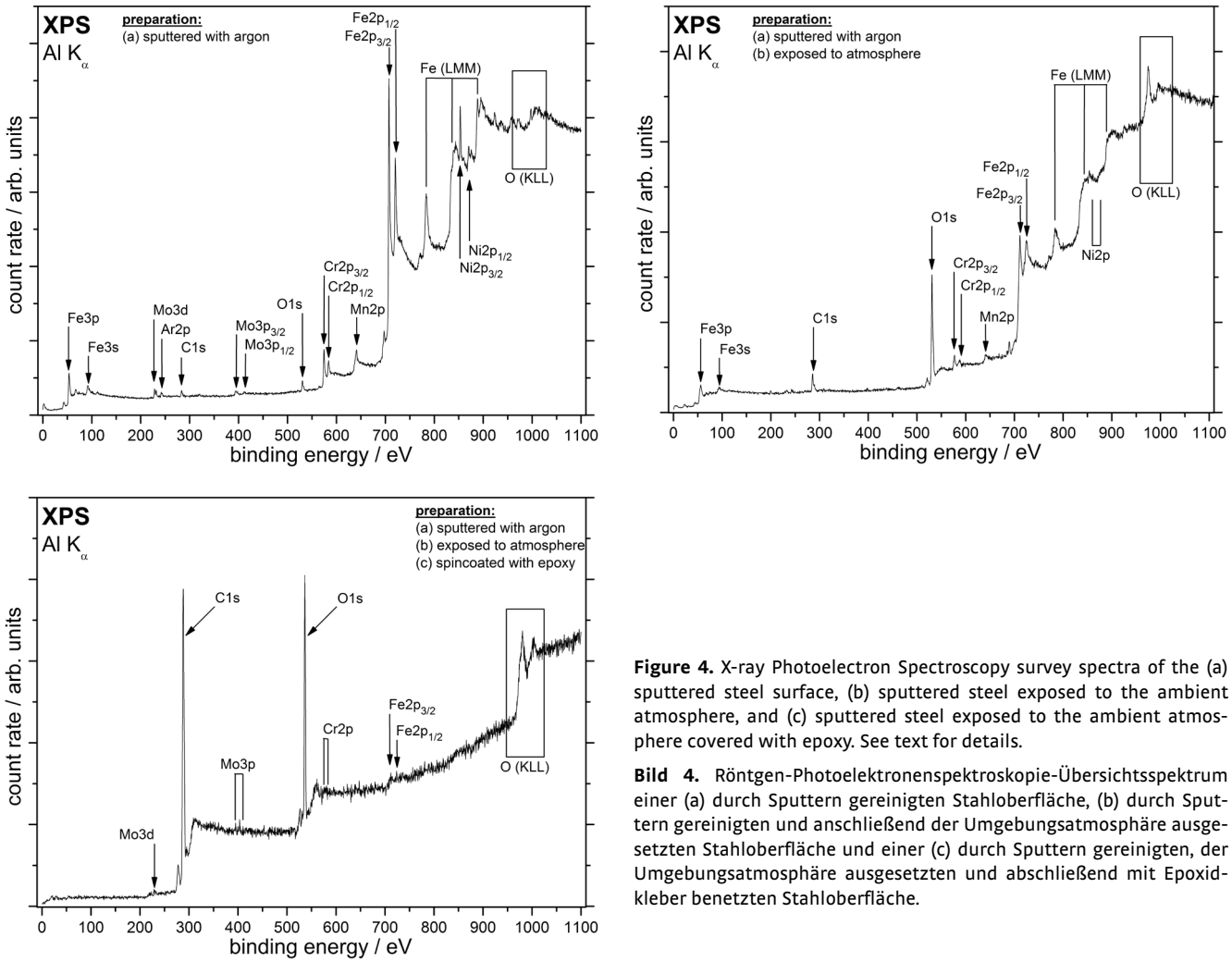

Figure 4. X-ray Photoelectron Spectroscopy survey spectra of the (a) sputtered steel surface, (b) sputtered steel exposed to the ambient atmosphere, and (c) sputtered steel exposed to the ambient atmosphere covered with epoxy. See text for details.

Bild 4. Röntgen-Photoelektronenspektroskopie-Übersichtsspektrum einer (a) durch Sputtern gereinigten Stahloberfläche, (b) durch Sputtern gereinigten und anschließend der Umgebungsatmosphäre ausgesetzten Stahloberfläche und einer (c) durch Sputtern gereinigten, der Umgebungsatmosphäre ausgesetzten und abschließend mit Epoxidkleber benetzten Stahloberfläche.

Table 3. After the cleaning procedure (a) bonds between carbon atoms at 285 eV (C_1, 38.1%) were found, which corresponds well to literature [20], Figure 5a. Carbon bound to metal, so-called carbide at 283.4 eV (C_0, 46.3%), thus with a chemical shift of ΔE = –1.6 eV referring to C_1, carbon with a single bond to oxygen (C-O) (C_2, 11.4%) at 286.5 eV (ΔE = 1.5 eV referring to C_1) and carbon double bound to oxygen (C=O) (C_3, 4.2%) at 287.9 eV (ΔE = 2.9 eV referring to C_1) are detected. All energetic positions and energy shifts correspond well to the literature [20]. The Full Width at Half Maximum (FWHM) of all peaks is fixed at 1.6 eV due to results from reference measurements. All results and values are comprised in Table 3.

After exposure to the ambient atmosphere (step (b)) a significant reduction of the carbide (C_0, 7.6%) at 283.8 eV, an increase of carbon-carbon bonds (C_1, 50.4%) at 285.6 eV and carbon single bound to oxygen (C-O) (C_2, 22.4%) at 287 eV were found. Furthermore a strong enhancement of the carbon double bound to oxygen (C=O) (C_4, 19.6%) at a higher binding energy (289.3 eV) is revealed.

The identified functional groups can be interpreted as ester compounds of carbon (C-O-C=O). Ester compounds have a typical binding energy fingerprint: The first binding energy is attributable to the C-O part (≈ 287.5 eV), the second binding energy to the O-C=O part (≈ 289.5 eV) [21]. Although after the first preparation step C=O compounds are to be found, however, no matching binding energy for potential O-C=O parts of ester compounds exist (C4 at 289.5 eV is missing), so that the identified substructures at 287.9 eV are attributable to ketones. The C-O peak at 286.5 eV is therefore not attributed to ester compounds, but originates from alcohols (C-OH) or ethers (C-O-C) [21].

The X-ray Photoelectron Spectroscopy detail spectra (c) of the C1s range of the epoxy covered surface is shown in Figure 5c. The structures can be identified as bonds between carbon atoms (C_1*, 54.2%) at 286.2 eV. Referring to C_1*, carbon single bound to oxygen (C-O) (C_2*) and carbon in an epoxy compound (C_3*) at 287.9 eV (38.0%) on the one hand and carbon double bound to oxygen (C=O) (C_4*) at 289.5 eV (7.8%) on the other hand can be identified [21].

The X-ray Photoelectron Spectroscopy detail spectra of the Fe2p range between 700 eV and 740 eV is shown in *Figure 6*. The relative contributions of these Fe2p spectra are summarized in *Table 4*.

The interpretation of X-ray Photoelectron Spectroscopy data appears to be quite complicated due to several possible oxidation

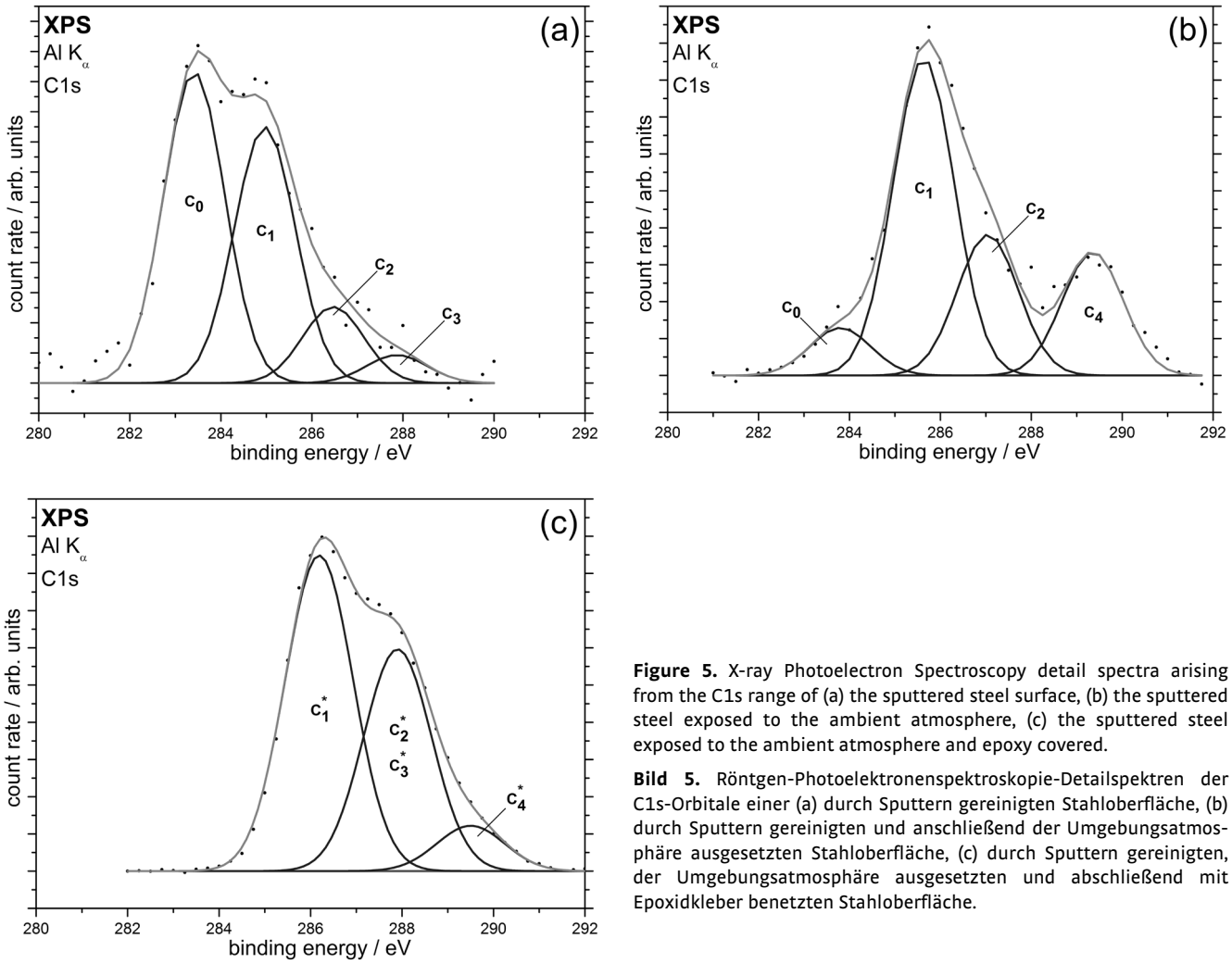

Figure 5. X-ray Photoelectron Spectroscopy detail spectra arising from the C1s range of (a) the sputtered steel surface, (b) the sputtered steel exposed to the ambient atmosphere, (c) the sputtered steel exposed to the ambient atmosphere and epoxy covered.

Bild 5. Röntgen-Photoelektronenspektroskopie-Detailspektren der C1s-Orbitale einer (a) durch Sputtern gereinigten Stahloberfläche, (b) durch Sputtern gereinigten und anschließend der Umgebungsatmosphäre ausgesetzten Stahloberfläche, (c) durch Sputtern gereinigten, der Umgebungsatmosphäre ausgesetzten und abschließend mit Epoxidkleber benetzten Stahloberfläche.

states, shake-up peaks, and the Fe2p spin-orbit splitting. Therefore, the present interpretation bases on the fundamental analysis of pure iron and well-defined iron oxides from previous works [16, 17]. The oxidation states Fe^0 at 707.5 eV ± 0.2 eV, Fe^{2+} at 710.1 eV ± 0.1 eV and Fe^{3+} at 711.1 eV ± 0.1 eV appear.

After the cleaning process (a) the metallic Fe^0 with 72.8% and the oxide Fe^{2+} with 27.2% were found, Figure 6a. The FWHMs are taken from literature and reference measurements [16].

After exposure to the ambient atmosphere (b) the metallic Fe^0 (15.3%) and the weakly oxidized Fe^{2+} (7.0%) are significantly reduced, Figure 6b. The main component is the strong Fe^{3+} contribution, which amounts to 77.7%. This means, that the surface is completely oxidized, because almost all iron atoms are in the Fe^{3+} state.

After the epoxy coverage of the the steel surface in step (c) the stoichiometry reveals that the amount of metallic Fe^0 remains almost unchanged, Figure 6c. A FWHM of 2.3 eV and a relative share of 13.3% resemble the values of the second step well (2.3 eV and 15.3%). It is surprising, that the contribution in the Fe^{3+} oxidation state is significantly reduced from 77.7% to 46.3% which is compensated by a rise of the Fe^{2+} contribution from 7.0% to 40.4%. This observation clearly shows that the epoxy interacts with the steel surfaces by reducing Fe^{3+} to Fe^{2+}. This is an evidence for strong chemical bonding between surface iron atoms and epoxy even before any activation as it is also carried out in the standard manufacturing process of the sandwich laminates [9, 10].

Table 4. Summarized values of all Fe2p-measurements (underlined values indicate assumed constraints).

Tabelle 4. Zusammenfassung der Fe2p-Messergebnisse (unterstrichene Werte kennzeichnen vorausgesetzte Zwangsbedingungen).

Preparation	Figure	Peak	Fe2p				Assignment
			$E_{binding}$ [eV]	ΔE	FWHM	rel. int.	
(a)	**6a**	**I**	707.3	0	2.2	72.8	Fe^0
		II	710.1	2.8	3.8	27.2	Fe^{2+}
		III	–	–	–	–	–
(b)	**6b**	**I**	707.7	0	2.3	15.3	Fe^0
		II	**710.1**	2.4	**3.9**	7.0	Fe^{2+}
		III	**711.1**	3.4	**3.9**	77.7	Fe^{3+}
(c)	**6c**	**I**	707.2	0	2.3	13.3	Fe^0
		II	**710.2**	3.0	**3.9**	40.4	Fe^{2+}
		III	**711.2**	4.0	**3.9**	46.3	Fe^{3+}

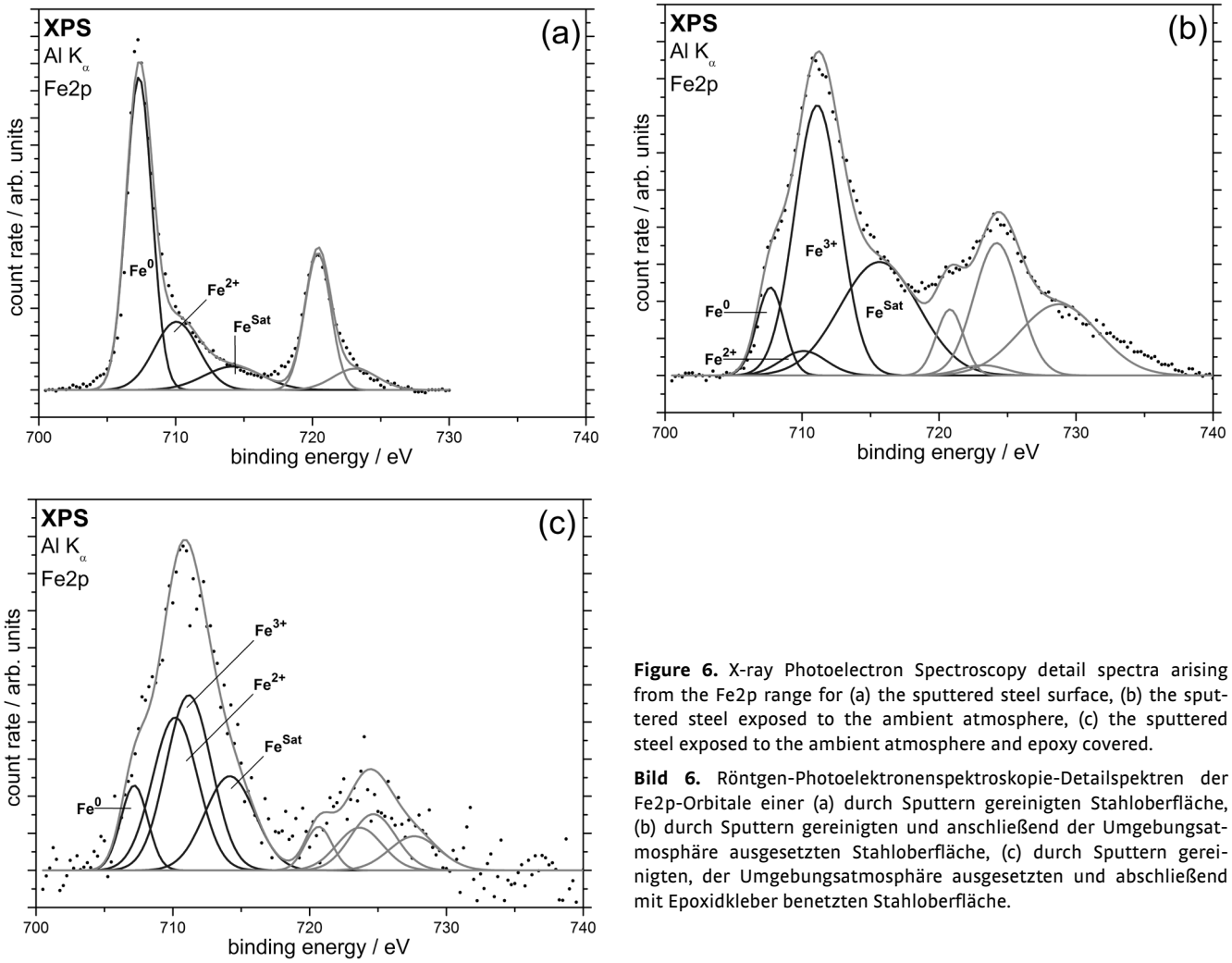

Figure 6. X-ray Photoelectron Spectroscopy detail spectra arising from the Fe2p range for (a) the sputtered steel surface, (b) the sputtered steel exposed to the ambient atmosphere, (c) the sputtered steel exposed to the ambient atmosphere and epoxy covered.

Bild 6. Röntgen-Photoelektronenspektroskopie-Detailspektren der Fe2p-Orbitale einer (a) durch Sputtern gereinigten Stahloberfläche, (b) durch Sputtern gereinigten und anschließend der Umgebungsatmosphäre ausgesetzten Stahloberfläche, (c) durch Sputtern gereinigten, der Umgebungsatmosphäre ausgesetzten und abschließend mit Epoxidkleber benetzten Stahloberfläche.

4 Conclusion

The present study explores insights into the adhesion mechanisms between stainless steel (316L) and industrial, polymeric epoxy adhesives. Topographical as well as chemical modifications are observed during the epoxy steel interaction applying Atomic Force Microscopy and X-ray Photoelectron Spectroscopy. It is shown that even very carefully cleaned steel surfaces under ultrahigh vacuum conditions still exhibit significant traces of carbon and oxygen.

Spin-coating the epoxy resin forms a layer on the steel surface including smooth regions as well as areas covered by clustered epoxy. X-ray Photoelectron Spectroscopy reveals the reduction of iron at the steel surface from Fe^{3+} to Fe^{2+} to a great extent, when coming into contact with the epoxy resin. This reduction occurs probably due to the interaction between the functional groups of the epoxy resin and iron oxides at the surface.

Acknowledgement

We gratefully acknowledge the provision of the DI3100 SPM (Prof. Daum) and the possibility to use the Omicron Multiprobe (Prof. Endres). We are thankful for the technical assistance by Christiane Jana Lehmann and Dana Schulte Genannt Berthold.

5 References

[1] G. Kickelbick, *Hybrid Materials – Synthesis, Characterization and Applications,* Wiley–VCH Verlag GmbH & Co. KGaA, Weinheim **2007**.

[2] L. Librescu, T. Hause, *Compos. Struct.* **2000**, *48*, 1.

[3] M. J. L. van Tooren, *A New Aircraft Material in Context,* Springer Science & Business Media B. V., Dordrecht **2004**.

[4] D. Zenkert, *The Handbook of Sandwich Construction,* Engineering Materials Advisory Services Limited (EMAS Ltd.), Worcester **1997**.

[5] D. Hull, T. W. Clyne, *An Introduction to Composite Materials,* Cambridge University Press, Cambridge **1996**.

[6] C. Bischof, A. Bauer, W. Possart, R. Kapelle, R. D. Schulze, *Acta Polym.* **1989**, *40*, 214.

[7] N. A. de Bruyne, *Aircraft Eng.* **1939**, *18*, 51.

[8] F. W. Reinhart, *J. Chem. Educ.* **1954**, *31*, 128.

[9] A. Carradò, O. Sokolova, B. Donnio and H. Palkowski, *J. Appl. Polym. Sci.* **2011**, *120*, 3709.

[10] J. Bishopp, Handbook of Adhesives and Sealants Volume 1 – Basic Concepts and High Tech Bonding, Elselvier Limited, Amsterdam **2005**.

[11] A. Carradò, J. Faerber, S. Niemeyer, G. Ziegmann, H. Palkowski, *Compos. Struct.* **2011**, *93*, 715.

[12] D. A. Shirley, *Phys. Rev. B* **1972**, *5*, 4709.

[13] J. H. Scofield, *J. Electron Spectr. Rel. Phenom.* **1976**, *8*, 129.

[14] M. P. Seah, W. A. Dench, *Surf. Interface Anal.* **1979**, *1*, 2.

[15] R. F. Reilman, A. Msezane, S. T. Manson, *J. Electron Spectr. Rel. Phenom.* **1976**, *8*, 389.

[16] K. Volgmann, F. Voigts, W. Maus-Friedrichs, *Surf. Sci.* **2010**, *604*, 906.

[17] T. Lin, G. Seshadi, J. Kelber, *Appl. Surf. Sci.* **1997**, *119*, 83.

[18] C. Leygraf, T. E. Gradel, *Atmospheric Corrosion,* Wiley-Interscience, New York **2000**.

[19] D. Lide, *Handbook of Chemistry and Physics – 79th Edition,* National Institute for Standards and Technology, Gaithersburg **1998**.

[20] L. Klarhöfer, B. Roos, W. Viöl, S. Dieckhoff, V. Kempter, W. Maus-Friedrichs, *Holzforschung* **2008**, *62*, 688.

[21] G. Beamson, D. Briggs, *High Resolution XPS of Organic Polymers – The Scienta ESCA-300 Database,* John Wiley & Sons Limited, Chichester **1992**.

Received in final form: December 21th 2012 T 51

